electronics

MDPI

Article

Design of 300 GHz Combined Doubler/Subharmonic Mixer Based on Schottky Diodes with Integrated MMIC Based Local Oscillator

José M. Pérez-Escudero [1,*], Carlos Quemada [1], Ramón Gonzalo [1,2] and Iñigo Ederra [1,2]

[1] Antenna Group, Public University of Navarra, 31006 Pamplona, Spain; carlos.quemada@unavarra.es (C.Q.); ramon@unavarra.es (R.G.); inigo.ederra@unavarra.es (I.E.)

[2] Institute of Smart Cities, Public University of Navarra, 31006 Pamplona, Spain

* Correspondence: josemanuel.perez@unavarra.es

Received: 5 November 2020; Accepted: 8 December 2020; Published: 10 December 2020

Abstract: In this paper the design and experimental characterization of a combined doubler-subharmonic mixer based on Schottky diodes which uses a 75 GHz MMIC based local oscillator is presented. This solution integrates in the same substrate the doubler and the mixer, which share the same metallic packaging with the local oscillator. The prototype has been fabricated and measured. For characterization, the Y-Factor technique has been used and the prototype yields a best conversion loss and equivalent noise temperature of 11 dB and 1976 K, respectively, at 305 GHz. This performance is close to the state of the art, and shows the potential of this approach, which allows a significant reduction in terms of size and volume.

Keywords: combined doubler/mixer; schottky diodes; THz

1. Introduction

For many decades the lack of efficient sources and detectors working in the submillimetre wave and terahertz ranges has led to the so-called THz-gap. However, the last decades have witnessed an unprecedented development of THz technology which has helped to bridge it. In the case of THz sources, advances in THz photonic and electronic technologies have enabled their development. To this end, two alternatives have been explored. The first one consists in using lower frequency electronic sources and then up-scale in frequency by means of multipliers. The second one involves the use of photonics sources and down-convert them to THz frequencies by means of photodiodes or photomixers [1,2]. At the beginning both approaches were independent; however, during the last decade the simultaneous use of photonic and electronic techniques has given rise to hybrid photonic-electronic devices. For example, the combination of Unitravelling Carrier Photodiodes (UTC-PD) and frequency multipliers has been proposed [3,4], and photonic techniques have been used for LO distribution [5], allowing to benefit from the best of both fields. Furthermore, progress in component integration has facilitated the design of submillimeter frequency multipliers and mixers, and therefore contributed to these advances [6–10].

Progresion has been largely motivated by the plethora of applications of THz technology: terahertz imaging, security, medical, radioastronomy or communications [11–17]. In this last case, these systems follow Edholm's law, which states that telecommunication data rates are as predictable as Moore's law, that is, the demand for point-to-point bandwidth in wireless communications doubles every 18 months [18]. The main advantage of THz communication links is the high data rate provided by the large bandwidth associated with such high frequencies. For this reason, THz links are postulated as a solution to palliate the problems of spectrum saturation and high data rate demand. Furthermore,

these links present other advantages such as lower susceptibility to scintillation effects than infrared wireless links and the possibility to use them for secure communications [19].

For these applications, receivers are usually based on Schottky diode mixers, which allow room temperature operation and fast modulation, which is a great advantage for high data rate links. In addition to this, Schottky diode mixers can be implemented in planar technology, which is of great interest since provide compact designs and enables integration with other components. In this work we propose a THz receiver which integrates not only a frequency multiplier and a subharmonic mixer but also a millimeter wave LO source. This LO source, which works around 77 GHz, consists of low-cost MMIC components inherited from the automotive radar industry. Therefore, the proposed configuration is a compact cost-effective solution, which, in terms of performance, behaves similar to a sub-harmonic mixer but in terms of frequency conversion is similar to a fourth harmonic mixer [10].

Several integrated THz receiver configurations have been proposed [20–26]. Nonetheless, in these designs the local oscillator is external, built as an independently packaged element. In the configuration presented in this work, the frequency doubler and subharmonic mixer are integrated on the same substrate, which makes it compatible with integrated Schottky diodes and simplifies assembly. Furthermore, the local oscillator is based on flip-chip MMICs and built on planar technology. Thus, all the circuits are integrated in a single metallic block, which eliminates the additional losses due to flange connections and misalignments produced in case of having external components, for example, the Local Oscillator. In addition such integration leads to significant reduction in mass and volume allowing, for example, the implementation multi-pixel arrays of heterodyne receivers for imaging applications [27].

The structure of the paper is organized as follows. First, Section 2 describes the proposed combined doubler/mixer with integrated MMIC local oscillator configuration, the design procedure and the predicted results. Afterwards, the manufacturing procedure and the experimental validation are presented in Section 3. Finally, conclusions are drawn in Section 4.

2. Design

The 3D whole model of the 300 GHz combined frequency doubler–subharmonic mixer with integrated local oscillator (LO) in a single packaging metallic block is shown in Figure 1.

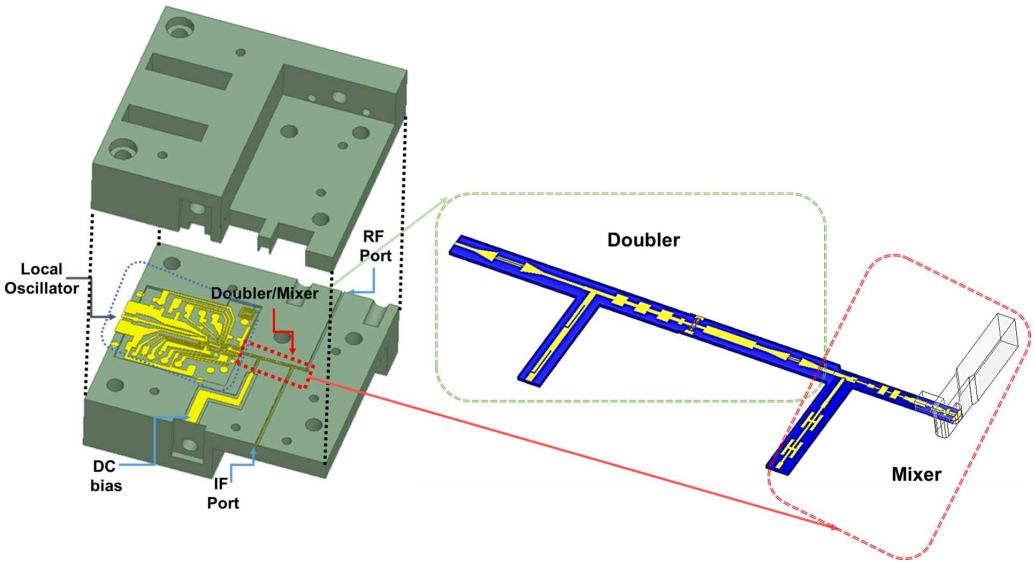

Figure 1. Explosion view of the 3D model of the combined doubler-subharmonic mixer with integrated MMIC based LO source. (Inset) 3D view of the combined doubler/harmonic mixer model without local oscillator for HFSS simulation.

The local oscillator source is composed of the following TriQuint flip-chip components [28]: a voltage-controlled oscillator (VCO) with 19 GHz output (TGV2204-FC) and two frequency doublers (TGC4703-FC and TGC4704-FC) in order to obtain a total frequency range from 74 GHz to 77 GHz with around 10 dBm output power. The material used to implement the printed circuit board (PCB) of this LO is Rogers 3210 ($\epsilon_r = 10.2,\ \tan\delta = 0.0027$). A schematic of this circuit can be seen in Figure 2.

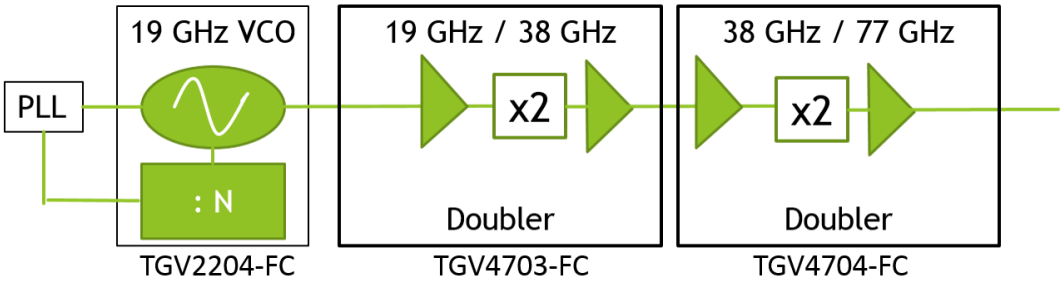

Figure 2. Schematic of the flip chip based source.

In order to accurately tune the LO output frequency and to stabilize the VCO, a 2.4 GHz Phase-Locked Loop (PLL) has been designed, based on the fractional frequency synthesizer ADF4158 from Analog Devices. This synthesizer provides 3 V maximum output voltage. Since the VCO control voltage is in the range from 0 to 8 V, an active loop filter with amplifiers has been used in order to obtain a higher voltage range. Thanks to it, the source output frequency, f_{IN}, can sweep the full 74 GHz to 77 GHz frequency range.

The source signal feeds a frequency doubler, which generates the LO signal for the subharmonic mixer. Thus, $f_{LO} = 2 \times f_{IN}$. The subharmonic mixer is based on an antiparallel Schottky diode pair, so that the even harmonics are suppressed by the configuration itself and the odd harmonics are, therefore, the only ones generated. The microstrip circuit is printed on 100 µm thick Cyclic Olefin Copolymer (COC) ($\epsilon_r = 2.3, \tan\delta = 0.0009$) [29,30]. This is a dielectric material with interesting properties, such as high chemical resistance, low water absorption, good metal adhesion, flexibility, low permittivity, and low losses in the THz region (0.1–10 THz) [31]. A schematic of the subharmonic mixer with integrated frequency doubler is shown in Figure 3. The radiofrequency signal is collected by a horn antenna (not shown) and then coupled from the input WR03 rectangular waveguide to a microstrip line. The frequency doubler uses four diodes antiseries chip with bias, which requires the use of additional DC-blocks.

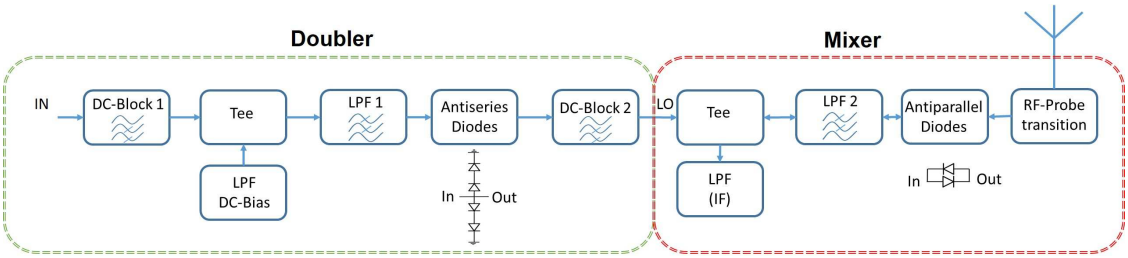

Figure 3. Schematic of the combined doubler/mixer circuit.

The local oscillator source is built on a different substrate (Rogers 3210) and wire bonded to the mixer substrate at the point IN in Figure 3. After the bonding that connects both substrates, a DC-block (DC-Block 1) is mandatory to avoid the DC bias of the frequency doubler diodes leaking to the MMIC source. In addition, the DC-bias path requires also a low-pass filter to avoid leakage of the source signal (LPF DC-bias) and a second DC-block at the doubler output (DC-Block 2). Finally, the multiplier also needs a low-pass filter (LPF 1) that lets the IN signal reach the diodes but rejects the doubler output, preventing it from reaching the MMIC source.

The subharmonic mixer is a standard subharmonic design. It requires a low pass filter (LPF 2), which lets the LO signal (i.e., the output of the doubler) pump the diodes and blocks the RF frequency. In addition, the waveguide probe that receives the RF signal and couples it to the microstrip line acts as a high-pass filter that rejects the lower frequency signals at the RF port. Finally, the IF output is formed by a tee with a low-pass filter for IF frequency, which blocks the RF and LO signals.

The design started with the frequency doubler as an independent device [32,33]. Afterwards, the subharmonic mixer was optimized, taking into account the output power of the doubler as the input LO of the mixer [34,35]. Once both designs have been finished, they are evaluated together.

2.1. Passive Circuit Design

The analysis of the different passive circuits, that is, filters, DC-blocks and transitions, is considered in this section. The software we have used for simulation is Ansys HFSS.

Firstly, the components of the frequency doubler are discussed. They are printed on 100 µm of Cyclic Olefin Copolymer (COC) ($\epsilon_r = 2.3, \tan\delta = 0.0009$) and placed inside a 340 µm width and 200 µm height air channel. This waveguide channel was included in the simulations of the filters. A top view of these elements, where the surrounding waveguide walls have been removed, and their predicted response are shown in Figure 4.

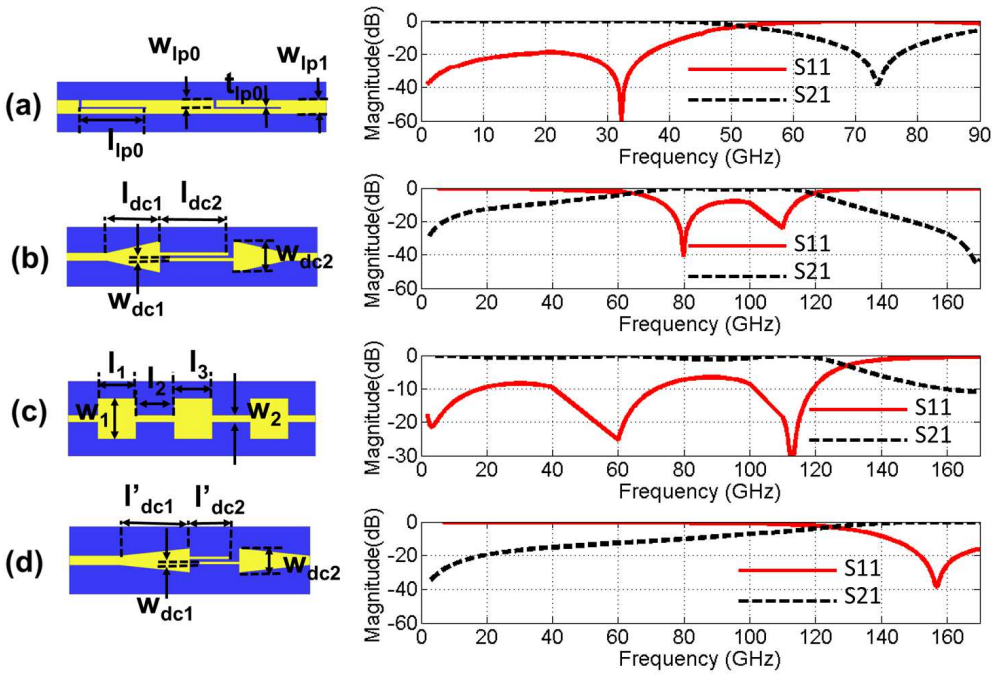

Figure 4. Top view and predicted response of the frequency doubler passive circuits: (**a**) Low pass filter for DC-Bias, (**b**) DC-Block 1 for IN frequency, (**c**) Stepped impedance low pass filter (LPF1) and (**d**) DC-Block 2 for LO frequency.

The first filter that can be observed, filter (a), is the low-pass filter for the DC-bias. The cut-off frequency, 50 GHz, allows the DC voltage to pass and provides around 25 dB rejection at IN frequency. The second filter, DC-Block 1, is a band-pass filter with 65 GHz cut-off frequency and 0.35 dB insertion loss at IN frequency. In Figure 4c we can see this stepped impedance low-pass filter. This kind of filter presents a great advantage for our design, since the required low impedance section widths are relatively narrow, which avoids higher order mode propagation in the channel. The rejection for LO is about 10 dB and the IN signal is in the pass-band with low insertion losses. Finally, the last filter, DC-block 2 (d), rejects the IN signal with more than 12 dB insertion loss and lets only the LO signal reach the subhamonic mixer circuit. The dimensions of all these circuits are compiled in Table 1.

Table 1. Dimensions of the passive circuits of the frequency doubler. See Figure 4, for reference.

Variable	Description	Dimensions (μm)	Variable	Description	Dimensions (μm)
l_{lp0}	Stub length	750	W_2	Step narrow width	30
w_{lp0}	Stub wide	100	l_1	Step length 1	250
t_{lp0}	Stub thick	20	l_2	Step length 2	280
w_{lp1}	Microstrip width	150	l_3	Step length 3	300
w_{dc1}	DC-Block width	30	w'_{dc1}	DC-Block width	30
w_{dc2}	DC-Block taper width	300	w'_{dc2}	DC-Block taper width	220
l_{dc1}	DC-Block taper length	500	l'_{dc1}	DC-Block taper length	500
l_{dc2}	DC-Block length	650	l'_{dc2}	DC-Block length	290
W_1	Step wide width	300			

The layout of the subharmonic mixer circuit components and its response is shown in Figure 5.

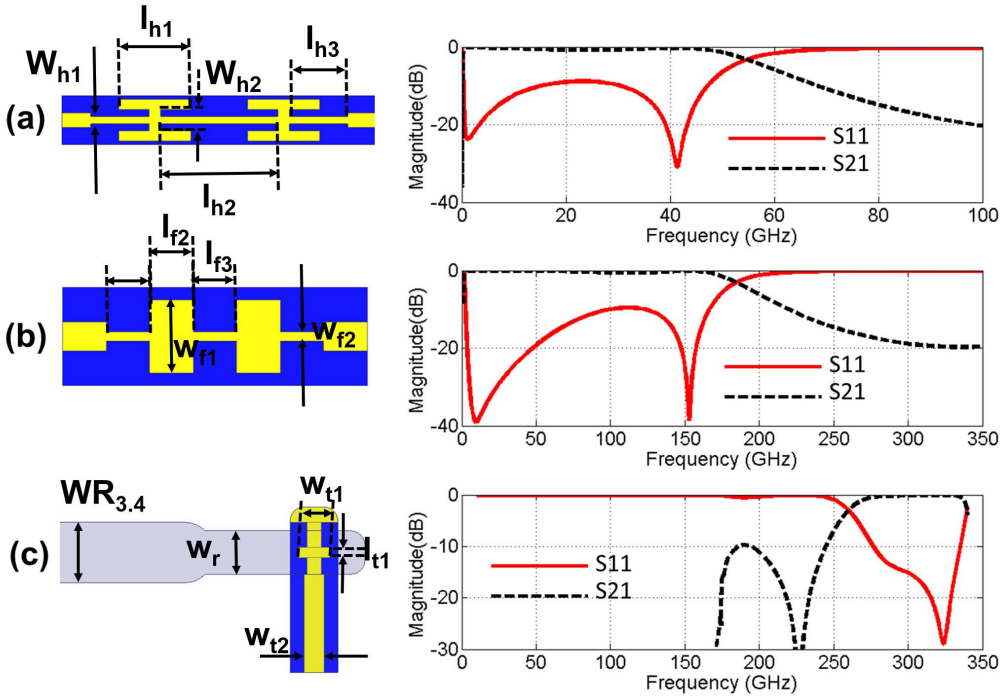

Figure 5. Top view and predicted response of passive circuits used in the subharmonic mixer: (**a**) IF Hammer-head filter, (**b**) Stepped impedance LPF for RF rejection and (**c**) RF E-Probe transition between waveguide and microstrip.

First, the IF output low-pass filter, which lets only the IF signal pass and rejects the higher frequencies, is shown in Figure 5a. The hammerhead configuration has been chosen because of its compactness and high rejection, about 20 dB for LO. The low-pass filter that rejects the RF signal is again a stepped-impedance low-pass filter, Figure 5b, whose rejection is 20 dB. The last element shown in Figure 5c is the waveguide probe that couples the RF signal to the microstrip. The probe is short-circuited, which provides the DC return for the diodes. Its insertion losses are lower than 0.5 dB from 276 GHz to 330 GHz. The dimensions of all these circuits are compiled in Table 2.

Table 2. Dimensions of the passive circuits of the subharmonic mixer . See Figure 5, for reference.

Variable	Description	Dimension (μm)
W_{h1}	Microstrip width	50
W_{h2}	Stub width	150
l_{h1}	Hammerhead length	500
l_{h2}	Hammerhead separation	820
l_{h3}	Microstrip length	410
l_{f1}	Step length 1	150
l_{f2}	Step length 2	170
l_{f3}	Step length 3	190
W_{f1}	Step wide width	250
W_{f2}	Step narrow width	30
w_{t1}	Patch width	220
l_{t1}	Patch length	70
w_{t2}	Microstrip width	140
w_r	waveguide match width	370
$wr_{3.4}$	Waveguide WR3.4 width	430

Finally, the length and width of the matching lines are calculated in order to adjust the diodes embedding impedance. This adjustment has been realized using the load-pull technique for best performance, that is, the minimum Conversion Loss (CL), at IN (75 GHz) and at LO (150 GHz) frequencies for the frequency doubler and at LO (150 GHz) and RF (300 GHz) for the subharmonic mixer.

2.2. Harmonic Balance

For the load pull analysis of the subharmonic mixer the impedances at LO and RF frequency have been calculated [36]. The minimum conversion losses of the mixer are obtained with diode embedding impedance $Z_{RF} = 28 + 11j$ and $Z_{LO} = 90.59 + 46.6j$ for RF and LO frequency, respectively. For the frequency doubler, the minimum conversion losses are obtained for diode embedding impedance $Z_{LO} = 90 + 86j$ and $Z_{IN} = 223 + 136j$ for LO and IN frequency, respectively. The diode bias was varied to optimize CL independently at each embedding impedance.

For the non-linear analysis we use the Schottky diode model from United Monolithic Semiconductors (UMS) foundry [37]. The resulting electrical characteristics for each diode are: an ideality factor $\eta = 1.2$, a saturation current $I_{sat} = 2 \times 10^{-16}$ A, an estimated resistance $R_S = 7.3\ \Omega$ and junction capacitance $C_j = 5.3$ fF for a 3μm length anode. The doubler and the mixer linear circuits are simulated separately, then the S-Parameters of the structure are imported to Keysight ADS software for the non-linear analysis.

For the frequency doubler analysis we have swept the input power from 6 dBm to 12 dBm, since the nominal output power of the 38 GHz Triquint TGV4704-FC frequency multiplier will be around 10 dBm. From the analysis realized in ADS we predicted the output power of the doubler and therefore its efficiency. These results are shown in Figure 6. The efficiency in this bandwidth is higher than 10 % for all cases. For 12, 10 and 8 dBm, where the output is around 4, 2 and 0 dBm, the efficiency is 15 %. For 6 dBm the output is around -3 dBm, therefore the efficiency is around 12 %. Thus, the doubler is narrow band but its bandwidth is enough for our design, since it covers the range of frequencies generated by the MMIC source. These results were obtained using -1.16 V DC bias.

On the other hand, in the subharmonic mixer case, -30 dBm RF input has been considered for the harmonic balance. The RF frequency has been swept, keeping the IF fixed to 2 GHz ($f_{RF} = 4f_{IN} + f_{IF} = 2f_{LO} + f_{IF}$). The mixer Local Oscillator is the output of the simulated doubler. Finally, the whole circuit is evaluated with HFSS and ADS combination for different power levels of the doubler local oscillator.

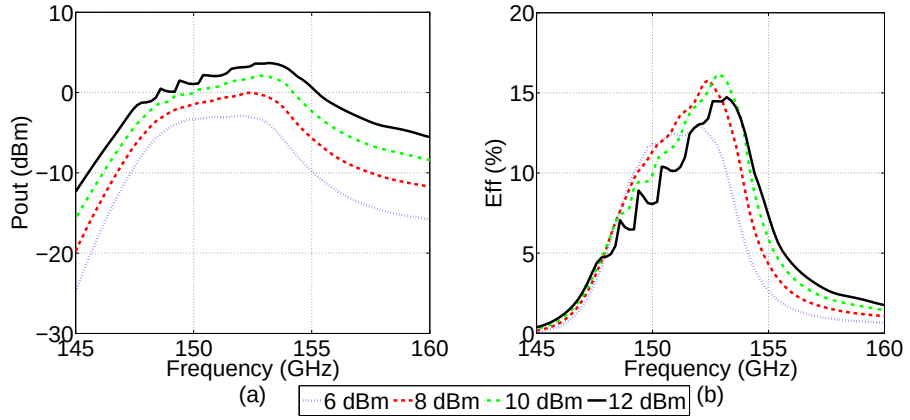

Figure 6. Predicted response of the frequency doubler for different IN input power levels: (**a**) Output power and (**b**) Efficiency.

The predicted results are shown in Figure 7. The conversion loss of the mixer for 12 dBm IN input power is around 8.5 dB from 300 GHz to 307 GHz and the mean value for the whole band, from 298 GHz to 310 GHz, is 9.6 dB. The mean DSB Equivalent Noise Temperature (ENT) is 1300 K. For 10 dBm IN Power the mean performance of the mixer in this frequency range is: 11 dB CL and 1900 K ENT. These values are similar to those shown in the literature. However, the performance of the mixer for 8 and 6 dBm IN power shows a significant degradation. For 8 dBm the conversion loss becomes 18.1 dB and the DSB ENT is 8100 K. For 6 dBm the mixer performance significantly degrades, the average DSB ENT increases to around 38,000 K and the CL to 23.8 dB. Summarizing, with enough power at the input, that is, more than 8 dBm, the doubler provides enough power to pump the subharmonic mixer. Otherwise, the performance significantly degrades.

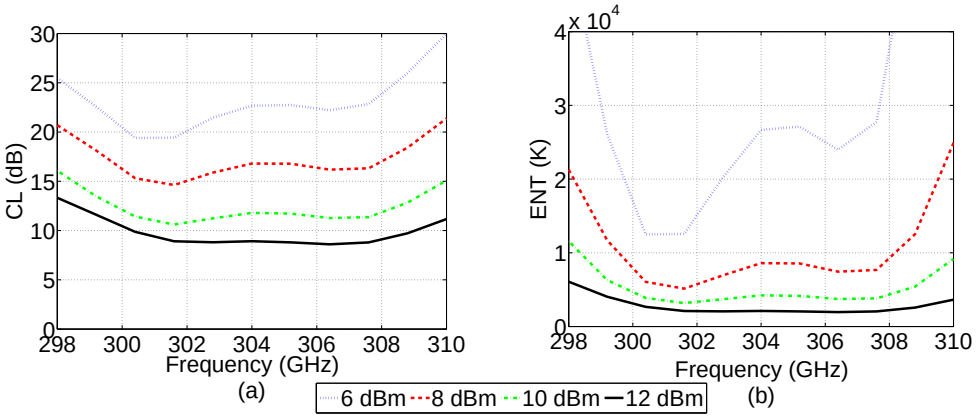

Figure 7. Predicted results of combined frequency doubler/subharmonic mixer for for different LO input power levels: (**a**) Conversion Loss and (**b**) DSB Equivalent Noise Temperature.

3. Manufacturing and Experimental Validation

The manufacturing process includes photolithography for the circuits on Rogers 3210 and Topas substrates and CNC machining for the housing metallic block. The photolithographic process was carried out in house. The metallic housing blocks were manufactured by CNC machining in a external workshop. Finally, the Schottky diodes were fabricated by United Monolithic Semiconductor (UMS) foundry. For the assembly, firstly the Schottky diodes were shaped using a Disco Dicing Saw DAD321. Once they have been cut they are epoxied to the microstrip circuit by means of silver epoxy (EPOTEK H20E). Silver epoxy and diodes placement were realized with a wire bonding and die placing machine (TPT HB16D) with an accuracy about 20 μm.

The local oscillator is fabricated on 670 µm thick Rogers 3210 by standard photolithography and cut with a LPKF H-100 milling machine. Its frequency is controlled by means of a Phase-Lock Loop. This PLL is mounted in a external board. The control voltage for the PLL are provided by an Arduino Due. Photographs of all these circuits are shown in Figure 8.

(**a**)

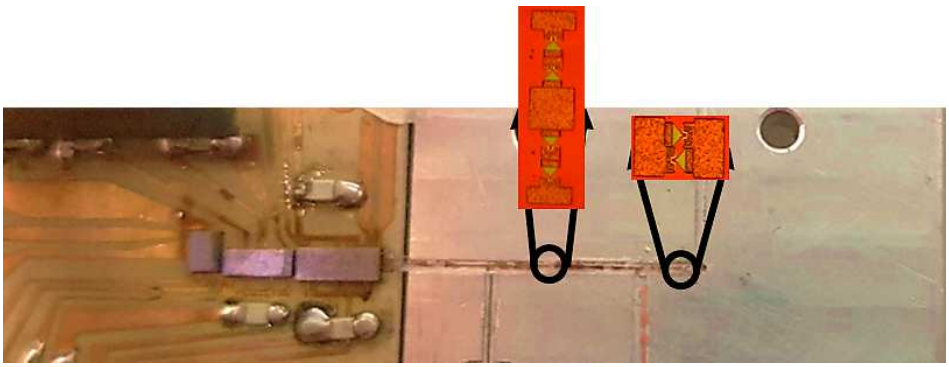

(**b**)

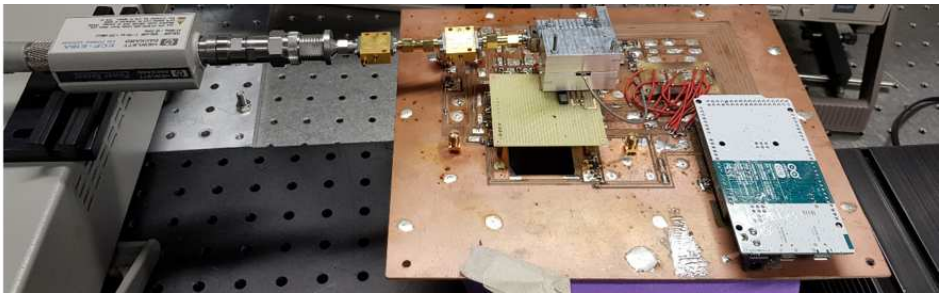

(**c**)

Figure 8. Photographs of: (**a**) (left) Prototype of local oscillator and (right) prototypes of doubler/mixer, IF hammerhead filter and LPF DC bias printed on Topas COC substrate with discrete diodes for size comparison; (**b**) Subharmonic mixer and the local oscillator in the enclosed metallic block with zoom of the UMS Schottky diodes and (**c**) Setup for Y-Factor measurement where the board with Arduino Due for LO tuning can be observed.

DC biasing for the frequency doubler was provided by a standard Power Supply. The IF chain consists of two LNA amplifiers (GAMP0100.0600SM10 [38,39]) with 35 dB gain and 1.8 dB NF. Their output was connected directly to a Keysight N9030A spectrum analyzer, where the power at 2 GHz was measured. A 20 dBi standard gain horn antenna was connected to the RF port of the mixer and the Y-Factor technique was applied using liquid Nitrogen and room temperature as as cold and hot loads respectively [40]. The photograph of the setup is shown in Figure 8c.

The values of conversion loss and equivalent noise temperature obtained by the Y-Factor measurement technique are compared with those predicted by simulation and shown in Figure 9a,b, respectively.

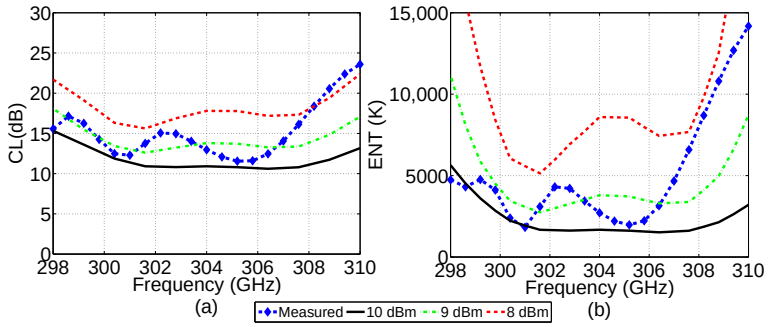

Figure 9. (**a**) Measured conversion loss of the integrated receiver subharmonic mixer and comparison with predicted performance. (**b**) Measured equivalent noise temperature of the integrated receiver subharmonic mixer and comparison with predicted performance.

The mean value of the measured ENT for the 298 GHz–310 GHz frequency range is 4876 K, which, compared with the simulations, is around twice higher than the predicted performance for 10 dBm LO power. The minimum ENT measured value is 1976 K, achieved at 305 GHz, and almost matches the simulated prediction. The same happens with the conversion losses, the measured mean value for the whole frequency range is 14.13 dB and at 305 GHz we obtain the best measured conversion loss, which is 11 dB. These results are about 3 dB higher than the predicted response where 10 dBm IN power was considered. However, if lower IN power is considered, the response matches the measurement results. That is why an additional comparison has been made with respect to the predicted simulated performance, since the measured response is in good agreement with the prediction for 9 dBm IN power, as shown in Figure 9a,b. This lower power can be explained by the additional losses in the manufactured circuit. Besides, the fact that the frequency doubler may be under-pumping the mixer diodes and that these diodes are manually epoxied would add additional losses. In addition to this, the power generated by the MMIC source is not constant in the working frequency band, which justifies the ripples in the experimental results and that the performance matches with simulated IN power in the range from 8 to 10 dBm. In spite of that, the behaviour is satisfactory and the results are not far from the the state-of-the-art.

4. Conclusions

A 300 GHz combined doubler/subharmonic mixer with integrated MMIC source has been designed and experimentally characterized. This cost effective solution allows the use of low frequency LO sources based on COTS components, which can be developed on planar technology. In addition, the integration of the doubler and the subharmonic mixer in the same substrate, allows all the receiver to be packaged in the same metallic housing.

A comparison between this work and other published mixers working at similar frequencies in terms of best and mean values of CL and ENT for the whole frequency range is shown in Table 3.

Table 3. State of the art of Schottky diode mixers working at similar frequencies to this work.

Ref	Frequency (GHz)	Mean CL (dB)	Mean ENT (K)	Best CL (dB)	Best ENT (K)
[9]	300–360	6.5	1270	5.7	1050
[20]	365–395	10	2500	7.5	1625
[35]	320–360	10	N.A	9	3300
[41]	360–395	N.A.	N.A.	10.9	3667
[42]	290–310	9.5	2300	9	2000
[43]	320–360	9	3000	6	1600
This Work	298–310	14.13	4876	11	1976

It can be observed that the results of this work are slightly higher than the state of the art. This is the price to be paid for the higher integration level with COST components, which limits the available IN power. As a matter of fact, the LO requirements of this design are similar to other subharmonic mixers, that is, 1.5–2.5 mW. However, the main difference is that this LO is generated by frequency multiplication of the integrated IN signal and the obtained LO level is lower than this value. Therefore, for a fair comparison, Reference [20] should be considered. This is also a combined doubler/mixer configuration, whose IN power level is about 80 mW, which is significantly higher than the IN level in this case, where the IN signal delivered to the doubler is lower than 30 mW.

The limitation on the performance of the device may be caused by different reasons: a lower output power of the MMIC source than predicted; the efficiency of the doubler is not very high so the diodes of the mixer may be under-pumped; the diodes are epoxied so that there is additional resistance and misalignment that provokes a little degradation. Moreover, the undesired electromagnetic interactions caused by the roughness and imperfections in the fabricated metallic packaging have not been taken into account in the simulations. Future versions would benefit from the use of integrated diode for the mixer/doubler, for example, using GaAs membrane technology. This higher integration could reduce present additional losses and would allow competing in performance with state-of-the-art devices, besides the LO generation integration advantage that this design presents.

Nonetheless, the presented results show the possibility of integration of a full THz receiver in the same single packaging metallic block, with the consequent reduction of mass and volume. Regarding volume, it is $4 \times 4.5 \times 2.4$ cm for the whole doubler/mixer prototype with the integrated signal generator (IN). Since our solution integrates the IN (and LO) signal generation, a direct comparison in these terms with other examples can not be performed, since these systems usually employ high power tunable laboratory sources for LO generation. As a matter of fact, this higher integration level is the main advantage of the proposed approach and pave the way for the design of compact 300 GHz receivers.

Author Contributions: Investigation: J.M.P.-E., C.Q., R.G., and I.E.; writing—original draft: J.M.P.-E.; writing—review & editing: I.E. All authors have read and agreed to the published version of the manuscript.

Funding: This research was funded by the Spanish MINECO, Project No. TEC2016-76997-C3-1-R, and by the Spanish State Research Agency, Project No. PID2019-109984RB-C43/AEI/10.13039/501100011033.

Conflicts of Interest: The authors declare no conflict of interest.

Abbreviations

The following abbreviations are used in this manuscript:

CL	Conversion Loss
COC	Cyclic Olefin Copolymer
COTS	Commercial Off-The-Shelf
DSB	Double Side Band
ENT	Equivalent Noise Temperature
IF	Intermediate Frequency
LO	Local Oscillator
MMIC	Monolithic microwave and integrated circuits
PLL	Phase-Locked Loop
UTC-PD	Unitravelling Carrier Photodiodes
VCO	Voltage Controlled Oscillator

References

1. Nagatsuma, T.; Ducournau, G.; Renaud, C.C. Advances in terahertz communications accelerated by photonics. *Nat. Photonics* **2016**, *10*, 371–379. [CrossRef]
2. Nagatsuma, T. Generating Millimeter and Terahertz Waves. *IEEE Microw. Mag.* **2009**, *10*, 64–74. [CrossRef]

3. Huggard, P.H.; Ellison, B.N.; Alderman, B.; Warner, J.E.J. 1.55 μm photomixer sources for mm-wave heterodyne detection and frequency conversion with Schottky diodes. In Proceedings of the Digest of the LEOS Summer Topical Meetings, San Diego, CA, USA, 25–27 July 2005; pp. 105–106, [CrossRef]
4. Ali, M.; Pérez-Escudero, J.M; Guzmán-Martínez, R.C.; Lo, M.-C.; Ederra, I.; Gonzalo, R. ; García-Muñoz, L.E.; Santamaría, G.; Segovia-Vargas, D.; van Dijk, F.; Carpintero, G. 300 GHz Optoelectronic Transmitter Combining Integrated Photonics and Electronic Multipliers for Wireless Communication. *Photonics* **2019**, *6*, 35. [CrossRef]
5. Torres-García, A.E; Pérez-Escudero, J.M.; Teniente, J.; Gonzalo, R.; Ederra, I. Silicon Integrated Subharmonic Mixer on a Photonic-Crystal Platform. *IEEE Trans. Terahertz Sci. Technol.* **2020**. [CrossRef]
6. Sobis, P. *Advanced Schottky Diode Receiver Front-Ends for Terahertz Applications*; Chalmers University of Technology: Gothenburg, Sweden, 2011.
7. Zhang, Y.; Zhao, W.; Wang, Y.; Ren, T.; Chen, Y. A 220 GHz subharmonic mixer based on schottky diodes with an accurate terahertz diode model. *Microw. Opt. Technol. Lett.* **2016**, *58*, 2311–2316. [CrossRef]
8. Wang, H. Conception et Modelisation de Circuits Monolithiques a Diode Schottky sur Substrat GaAs aux Longueurs d'onde Millimetriques et Submillimetriques pour les Recepteurs Heterdodynes Multi-Pixels Embarques sur Satellites et Dedies a L'Aeronomie ou la Planetologie. Ph.D. Thesis, Observatoire de Paris, Paris, France, 2009.
9. Thomas, B. ; Maestrini, A.; Beaudin, G. A low-noise fixed-tuned 300-360-GHz sub-harmonic mixer using planar Schottky diodes. *IEEE Microw. Wireless Comp. Lett.* **2005**, 15, 865–867. [CrossRef]
10. Maestrojuan, I.; Ederra, I.; Gonzalo, R. Fourth-Harmonic Schottky Diode Mixer Development at Sub-Millimeter Frequencies. *IEEE Trans. Terahertz Sci. Technol.* **2015**, 5, 518–520. [CrossRef]
11. Hasch, J.; Topak, E.; Schnabel, R.; Zwick, T.; Weigel, R.; Waldschmidt, C. Millimeter-Wave Technology for Automotive Radar Sensors in the 77 GHz Frequency Band. *IEEE Trans. Microw. Theory Tech.* **2012**, *60*, 845–860. [CrossRef]
12. Yujiri, L.; Shoucri, M.; Moffa, P. Passive Millimeter-Wave Imaging. *IEEE Microw. Mag.* **2003**, *4*, 39–39. [CrossRef]
13. Panzner, B. In-band wireless backhaul for 5G millimeter wave cellular communications-interactive live demo. In Proceedings of the IEEE Conference on Computer Communications Workshops Hong Kong, Hong Kong, China, 26 April–1 May 2015; pp. 21–22.
14. Golcuk, F.; Kanar, T.; Rebeiz, G.M. A 90–100 GHz 4x4 SiGe BiCMOS Polarimetric Transmit/Receive Phased Array with Simultaneous Receive-Beams Capabilities. *IEEE Trans. Microw. Theory Tech.* **2013**, *61*, 3099–3114. [CrossRef]
15. Folster, F.; Rohling, H.; Lubbert, U. An Automotive Radar Network Based on 77 GHz FMCW sensors. Proceedings of the IEEE International Radar Conference, Arlington, VA, USA, 9–12 May 2005; pp. 871–876.
16. Sheen, D. M.; McMakin, D. L.; Hall, T. E. Three-dimensional millimeter-wave imaging for concealed weapon detection. *IEEE Trans. Microw. Theory Tech.* **2001**, *49*, 1581–1592. [CrossRef]
17. Torres-García, A. E.; Ederra, I.; Gonzalo, R. Implementation of a THz quasi-spiral antenna for THz-IR detector. In Proceedings of the 11th European Conference on Antennas and Propagation (EUCAP), Paris, France, 19–24 March 2017; pp. 2526–2529.
18. Edholm's Law of Bandwidth. Available online: http://spectrum.ieee.org/telecom/wireless/edholms-law-of-bandwidth (accessed on 9 May 2017).
19. Federici, J.; Moeller, L. Review of terahertz and subterahertz wireless communications. *J. Appl. Phys.* **2010**, *107*, 13–26. [CrossRef]
20. Thomas, B.; Alderman, B.; Matheson, D.; de Maagt, P. A Combined 380 GHz Mixer/Doubler Circuit Based on Planar Schottky Diodes. *IEEE Microw. Wirel. Components Lett.* **2008**, *18*, 353–355. [CrossRef]
21. Treuttel, J.; Maestrini, A.; Alderman, B.; Wang, H.; de Maagt, P. Design of a combined tripler-subharmonic mixer at 330 GHz for multipixel application using European Schottky diodes. In Proceedings of the 21st International Symposium on Space Terahertz and Technology, Oxford, UK, 23–25 March 2010
22. Ederra, I.; Azcona, L.; Alderman, B.E.J.; Laisné, A.; Gonzalo, R.; Mann, C.M.; Matheson, D.N.; de Maagt, P. A 250 GHz Sub-Harmonic Mixer Design Using EBG Technology. *IEEE Trans. Antennas Propag.* **2007**, *55*, 2974–2982. [CrossRef]
23. Khromova, I.; Gonzalo, R.; Ederra, I.; Delhote, N.; Baillargeat, D.; Murk, A.; Alderman, B.; de Maagt, P. Subharmonic Mixer Based on EBG Technology. *IEEE Trans. Terahertz Sci. Technol.* **2013**, *3*, 838–845. [CrossRef]

24. Reck, T.; Jung-Kubiak, C.; Siles, J. V.; Lee, C.; Lin, R.; Chattopadhyay, G.; Mehdi, I.; Cooper, K. A Silicon Micromachined Eight-Pixel Transceiver Array for Submillimeter-Wave Radar. *IEEE Trans. Terahertz Sci. Technol.* **2015**, *5*, 197–206. [CrossRef]
25. Thomas, B.; Lee, C.; Peralta, A.; Gill, J.; Chattopadhyay, G.; Sin, S.; Lin, R.; Mehdi, I. A 530–600 GHz Silicon Micro-machined Integrated Receiver Using GaAs MMIC Membrane Planar Schottky Diodes. In Proceedings of the 21st International Symposium on Space Terahertz Technology, Oxford, UK, 23–25 March 2010.
26. Maestrini, A.; Thomas, B.; Wang, H.; Jung, C.; Treuttel, J.; Jin, Y.; Chattopadhyay, G.; Mehdi, I.; Beaudin, G. Schottky diode-based terahertz frequency multipliers and mixers. *C. R. Phys.* **2010**, *11*, 480–495. [CrossRef]
27. Wang, H. ; Maestrini, A.; Thomas, B.; Alderman, B.; Beaudin, G. Development of a Two-Pixel Integrated Heterodyne Schottky Diode Receiver at 183 GHz.In Proceedings of the 9th International Symposium on Space Terahertz Technology, Groningen, The Netherlands, 28–30 April 2008.
28. Automotive. Available online: https://www.qorvo.com/applications/automotive (accessed on 4 August 2017).
29. Maestrojuan, I.; Palacios, I.; Ederra, I.; Gonzalo, R. Use of COC substrates for millimeter-wave devices. *Microw. Opt. Technol. Lett.* **2014**, *57*, 371–377. [CrossRef]
30. Rebollo, A. Development of an Auto-Calibrated Receiver in Planar Technology at Millimetre-Wave Frequencies. Ph.D. Thesis, Universidad Pública de Navarra, Pamplona, Spain, 2015
31. Sengupta, A.; Bandyopadhyay, A.; Bowden, B.F.; Harrington, J.A.; Federici, J.F. Characterisation of olefin copolymers using tera-hertz spectroscopy. *Electron. Lett.* **2006**, *42*, 1477–1479. [CrossRef]
32. Chen, Z.; Wang, H. ; Alderman, B.; Huggard, P. ; Zhang, B.; Fan, Y. 190 GHz high power input frequency doubler based on Schottky diodes and AlN substrate. *IEICE Electron. Express* **2016**. [CrossRef]
33. Zhao, C. Modelling and Characterisation of a Broadband 85/170 GHz Schottky Varactor Frequency Doubler. Ph.D. Thesis, Chalmers University of Technology, Gothenburg, Sweden, 2011.
34. Mehdi, I.; Marazita, S.M. Improved 240-GHz subharmonically pumped planar Schottky diode mixers for space-borne applications. *IEEE Trans. Microw. Theory Tech.* **1998**, *46*, 2036–2042. [CrossRef]
35. Thomas, B.; Rea, S.; Moyna, B.; Alderman, B.; Matheson, D. A 320–360 GHz Subharmonically Pumped Image Rejection Mixer Using Planar Schottky Diodes. *IEEE Microw. Wirel. Comp. Lett.* **2009**, *19*, 101–103. [CrossRef]
36. Hesler, J.L. Planar Schottky Diodes in Submillimeter-Wavelength Waveguide Receivers. Faculty of the School of Engineering and Applied Science of the University of Virginia. Ph.D. Thesis, University of Virginia, Charlottesville, VA, USA, 1996.
37. Technologies. Available online: https://www.ums-gaas.com/foundry/technologies/ (accessed on 21 October 2016).
38. GAMP0100.0600SM10. Available online: http://www.myneotech.com/products/gamp0100-0600sm10/ (accessed on 10 March 2018).
39. Vizard, D.R.; Foster, P. R. ; Lunn, B. ; Cherry, S. M. Full coverage millimetre wave primary noise standards for 18-170 GHz. In Proceedings of the 2008 IEEE MTT-S International Microwave Symposium Digest, Atlanta, GA, USA, 15–20 June 2008; pp. 1537–1540.
40. Maestrojuan, I.; Rea, S.; Ederra, I.; Gonzalo, R. Experimental analysis of different measurement techniques for characterization of millimeter-wave mixers. *Microw. Opt. Tech. Lett.* **2014**, *56*, 1441–1447. [CrossRef]
41. Treuttel, J.; Thomas, B.; Maestrini, A. ; Wang, H. ; Alderman, B.; Siles, J.V. ; Davis, S.; Narhi, T. A 380 GHz sub-harmonic mixer using MMIC foundry based Schottky diodes transferred onto quartz substrate. In Proceedings of the 20th International Symposium on Space Terahertz Technology, Charlottesville, VA, USA, 20–22 April 2009.
42. Guo, C.; Shang, X.; Lancaster, M.J.; Xu, J.; Huggard, P.G. A 290–310 GHz Single Sideband Mixer with Integrated Waveguide Filters. *IEEE Trans. Terahertz Sci. Technol.* **2018**, *8*, 446–454. [CrossRef]
43. Sobis, P. J.; Emrich, A.; Stake, J. A Low VSWR 2SB Schottky Receiver. *IEEE Trans. Terahertz Sci. Technol.* **2011**, *1*, 403–411. [CrossRef]